RAPID COMMUNICATIONS

PHYSICAL REVIEW A VOLUME 44, NUMBER 3 1 AUGUST 1991

Alignment effects of $|J=3\rangle$ states prepared by three-photon excitation: Sixfold symmetry in collisional energy transfer, $Ca(4s4f, {}^1F_3)+He \rightarrow Ca(4p^2, {}^1S_0)+He$

Jan P. J. Driessen, Christopher J. Smith, and Stephen R. Leone*

Joint Institute for Laboratory Astrophysics, National Institute of Standards and Technology and University of Colorado, Department of Chemistry and Biochemistry, and Department of Physics, University of Colorado, Boulder, Colorado 80309-0440

(Received 15 January 1991)

Rank-6 symmetry in energy-transfer collisions is observed. A $Ca(4s4f, {}^1F_3)$ state is prepared by three-photon excitation. The angular wave function of the $Ca({}^1F_3)$ state depends on the angles of the three laser polarizations with respect to each other. The alignment effect for energy transfer, $Ca(4s4f, {}^1F_3)+He \rightarrow Ca(4p^2, {}^1S_0)+He$, is determined for two different initial angular wave functions. Each alignment curve can be analyzed in terms of the same set of relative cross sections for the individual $Ca({}^1F_3)$ magnetic sublevels, providing an independent verification of the data.

Orbital alignment effects for inelastic collisions of atoms have been the focus of attention by numerous experimentalists and theorists [1–22]; a great deal of new information about potential-energy surfaces and collision dynamics can be revealed. To appreciate the wealth of information in this field, the reader is referred to reviews by Hertel *et al.* [23], and by Campbell, Schmidt, and Hertel [24]. Typically, an aligned state is prepared using a linearly polarized laser beam, after which the atom collides with an atomic or molecular partner and changes state. The laser polarization serves as the quantization axis for the excited state. The relevant quantization axis for the collision process, however, is the relative velocity vector ($\mathbf{v}_{rel}$), which makes an angle β with respect to the laser quantization axis. The observed cross section $\sigma(\beta)$ for integer total angular momentum states has the general form

$$\sigma(\beta)=\sum_{n=0}^{J} a_{2n}\cos(2n\beta)\,, \tag{1}$$

with J representing the total angular momentum of the aligned state(s). The simplest form of Eq. (1) is obtained for atomic P states ($J=1$), resulting in a pure $\cos(2\beta)$ dependence. The majority of alignment experiments have studied this angular behavior. In experimental studies of collision events between two aligned P states [7,9], an angular dependence up to the $\cos(4\beta)$ term has been demonstrated. This angular behavior has also been observed in alignment studies involving atomic states with total angular momentum $J\geq 2$ [15–17,19].

In this paper we report the use of three linearly polarized laser beams to prepare an aligned $Ca(4s4f, {}^1F_3)$ state with total angular momentum $J=3$, in which the $\cos(6\beta)$ term may be observed. We measure the angular dependence of the cross section for near-resonant energy transfer in the collision process

$$Ca(4s4f, {}^1F_3)+He \rightarrow Ca(4p^2, {}^1S_0)+He+\Delta E=557\ cm^{-1}. \tag{2}$$

The angular wave function of the aligned $Ca(4s4f, {}^1F_3)$ state depends on the angles of the individual laser polarizations with respect to each other. Two polarization configurations are chosen, for which the angular dependence of the cross section is measured. With all three laser polarizations parallel (↕↕↕), the $Ca(4s4f, {}^1F_3)$ state is prepared with an angular wave function $Y_{3,0}$ where the laser polarization vectors serve as the quantization axis. By choosing one laser polarization perpendicular to the other two laser polarizations (↔↕↕), an aligned state with angular wave function $(Y_{3,-1}-Y_{3,1})/\sqrt{2}$ is prepared with respect to the two parallel laser polarizations. These two states show very different alignment behavior and angular terms up to $\cos(6\beta)$ according to Eq. (1) are observed in a collision process.

Figure 1 shows the energy-level diagram of the calcium system. The $Ca(4s4f, {}^1F_3)$ state is excited in three steps via the singlet-P ($S\rightarrow P$: 422.7 nm) and the singlet-D levels ($P\rightarrow D$: 732.6 nm), using three collinearly propagating pulsed dye laser beams. The third excitation step ($D\rightarrow F$) is realized by a 1981.5-nm photon, which is produced by Raman shifting a visible laser beam (748.6 nm) in hydrogen and selecting the second Stokes line with a dispersing prim. A single neodymium-doped yttrium aluminum garnet (Nd:YAG) laser is used to pump all three pulsed dye lasers, in order to guarantee the time overlap of the three laser pulses at the scattering center and thus to ensure the stability of the excitation amplitude of the $^1F_3$ state. The linear polarization of each of the three laser beams is refined using Glan laser prisms and the polarization of one laser is rotated over 90°, when necessary, using a double-Fresnel-rhomb polarization rotator. The laser polarizations can thus be fixed relative to each other to produce the previously mentioned configurations, preparing either the angular wave function $Y_{3,0}$ or $(Y_{3,-1}-Y_{3,1})/\sqrt{2}$. A second double-Fresnel-rhomb rotator is used to rotate all three laser polarizations simultaneously, and measurements of the energy-transfer process are made every 10°. The rotator basically functions as a half-wave retarder over a very broad wavelength region (330–1100 nm). However, for the 1981.5-nm laser beam, the retardation is $\approx 173°$ instead of the ideal 180°. This effect produces a slight ellipticity in the polarization of the 1981-nm beam as it is rotated over 90°. In the parallel configuration (↕↕↕) this ellipticity is removed by using a Glan laser prism after the double-rhomb rotator to

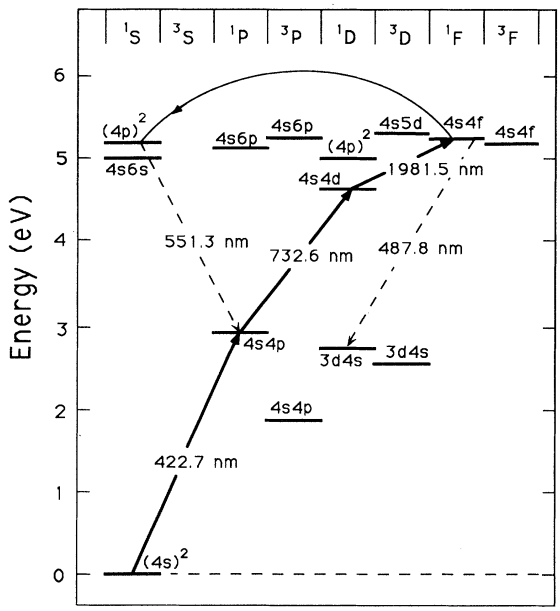

FIG. 1. The relevant energy levels in the calcium atom. The levels are arranged in $^{(2S+1)}L$ groups, as shown at the top of the figure. The triplet degeneracy is too small to be shown on this scale. The laser transitions for the $^1F_3$ excitation are indicated by the thick arrows. The dashed arrows indicate the decay transitions of the $^1F_3$ and the $^1S_0$ state that are monitored in the collision process.

clean up the polarizations. In the perpendicular configuration ($\leftrightarrow\updownarrow$), this cannot be done. Therefore, the ellipticity is taken into account in the analysis of the perpendicular data. A detailed discussion of this effect will be presented in the future [25].

The experimental configuration consists of a crossed-beam apparatus, as described previously [14,17]. The average relative velocity vector is well known. The small angular spread of the velocity vector ($\Delta\beta \approx 15°$) is found to have a negligible effect on our final results. The laser polarizations rotate in the collision plane, defined by the two atomic beams. A small fraction ($\leq 1\%$) of the excited Ca($^1F_3$) population is collisionally transferred to the nearby Ca($4p^2$, $^1S_0$) state. Fluorescence from this state is collected at 551.3 nm with a fiber-optic bundle which is positioned to maximize the solid angle of acceptance. Because of the isotropic character of the final state ($^1S_0$), there is no anisotropy in the emitted fluorescence of this state. The collected fluorescence light from the interaction center is sent through a 0.5-m monochromator in combination with a bandpass filter and detected by a photomultiplier tube (PMT). In this manner we count the 551.3-nm photons, and thus the relative number of collisionally produced Ca($^1S_0$) is monitored. The use of the filter is found to improve the signal-to-background ratio by a factor of 5. To monitor the initial $^1F_3$ state, a second fiber-optic bundle collects fluorescence light from the interaction region. This fluorescence is selected with a bandpass filter at 487.8 nm (9 nm full width at half maximum) and is detected by a second PMT. The PMT current is integrated by a boxcar and converted to counts by a voltage-to-frequency convertor. There is no angular structure in the initial-state signal because of the large solid angle of collection. The $^1F_3$ signal varies less than 5% due to thermal drift of laser frequencies and Ca beam intensity. The ratio of the $^1S_0$ signal to the $^1F_3$ signal is proportional to the cross section. This ratio is measured over a large angular range, giving us the alignment data. The background signals due to laser scatter, stray room light, and PMT dark counts are accounted for by subtracting the $^1S_0$-to-$^1F_3$ ratio as measured with the rare-gas beam off at each angle.

The measuring time includes 3000 (1000) laser pulses with the rare-gas beam on (off) and the YAG laser running at 10 Hz. A range of 23 angles is measured in steps of 10°. Five such runs are averaged together, giving small statistical error bars. Thus typical measuring times are 14 h per alignment curve.

The observed alignment data are shown in Fig. 2 for both parallel ($\updownarrow\updownarrow$) and perpendicular ($\leftrightarrow\updownarrow$) laser polarizations. The angular behavior of the cross section, given by Eq. (1), can be rewritten in a semiclassical description as follows [17]:

$$\sigma(\beta) = \sum_M \left| \sum_{M'} p_{M'} d^J_{MM'}(\beta) \right|^2 \sigma^{|M|}, \tag{3}$$

where M is the component of J along the relative velocity

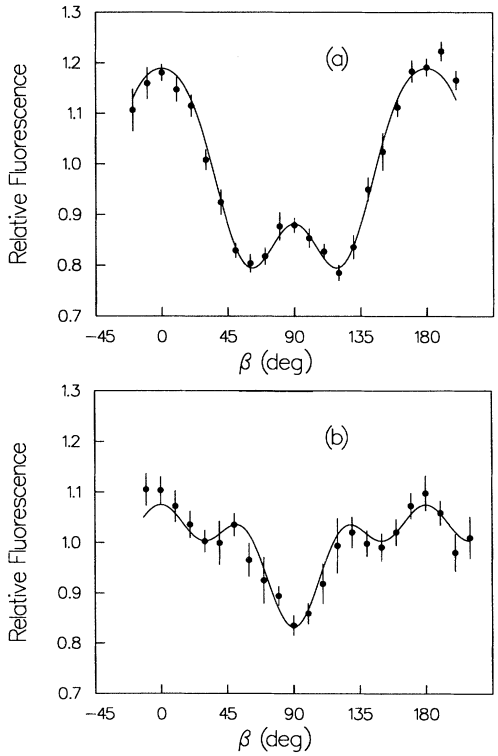

FIG. 2. Alignment data for energy transfer of Ca($4s4f$, $^1F_3$) with He. The relative fluorescence of the collisionally produced Ca($4p^2$, $^1S_0$) state is shown as a function of the angle β. (a) Laser polarizations fixed parallel to one another ($\updownarrow\updownarrow\updownarrow$: $Y_{3,0}$); (b) one laser polarization perpendicular to the other two [$\leftrightarrow\updownarrow$: $(Y_{3,-1} - Y_{3,1})/\sqrt{2}$].

vector, M' is the component of J along the laser polarization vector, the Wigner d functions $d^J_{MM'}(\beta)$ are rotation matrices [26] which relate the quantization axes of the laser and collision frames, and $p_{M'}$ are the expansion coefficients of the angular wave functions in terms of its eigenfunctions $Y_{l,m}$ [parallel ($\updownarrow\updownarrow\updownarrow$): $p_{M'}=\delta_{M',0}$; perpendicular ($\leftrightarrow\updownarrow\updownarrow$): $p_{M'}=(\delta_{M',-1}-\delta_{M',1})/\sqrt{2}$]. The total cross section is sensitive exclusively to diagonal elements of the atomic density matrix, since the azimuthal dependence of the off-diagonal elements [$\exp(-i(M-M')\phi)$] averages to zero when integrated over the whole impact-parameter range. The $\sigma^{|M|}$ are the total cross sections for collisionally induced electronic energy transfer from an individual sublevel (M) of the initial $Ca(^1F_3)$ state to the $^1S_0$ state. These individual M-state cross sections are averaged over impact parameter and azimuthal angle. Because Eqs. (1) and (3) represent the same alignment dependence, we can express the a_{2n} coefficients in terms of the individual sublevel cross sections $\sigma^{|M|}$. For the parallel configuration ($\updownarrow\updownarrow\updownarrow$), this expression is given by

$$\begin{pmatrix} a_0 \\ a_2 \\ a_4 \\ a_6 \end{pmatrix} = \frac{1}{256} \begin{pmatrix} 68 & 78 & 60 & 50 \\ 78 & 27 & -30 & -75 \\ 60 & -30 & -60 & 30 \\ 50 & -75 & 30 & -5 \end{pmatrix} \begin{pmatrix} \sigma^0 \\ \sigma^{|1|} \\ \sigma^{|2|} \\ \sigma^{|3|} \end{pmatrix} . \quad (4)$$

For the perpendicular configuration ($\leftrightarrow\updownarrow\updownarrow$) we find this expression to be

$$\begin{pmatrix} a_0 \\ a_2 \\ a_4 \\ a_6 \end{pmatrix} = \frac{1}{512} \begin{pmatrix} 156 & 226 & 100 & 30 \\ 54 & 31 & -70 & -15 \\ -60 & 30 & 60 & -30 \\ -150 & 225 & -90 & 15 \end{pmatrix} \begin{pmatrix} \sigma^0 \\ \sigma^{|1|} \\ \sigma^{|2|} \\ \sigma^{|3|} \end{pmatrix} . \quad (5)$$

By performing a least-squares analysis of Eqs. (1) and (3) to the alignment curves, we are able to determine the relative cross sections $\sigma^{|M|}$ as well as the expansion coefficients a_{2n}. The results of these fits are given in Table I. We observe a distinct $\cos(6\beta)$ dependence for the perpendicular case ($\leftrightarrow\updownarrow\updownarrow$). The individual fitting results of the two alignment curves are given in the first two columns. The error bar in the $\sigma^{|3|}$ parameter is larger in the perpendicular case, because the $\sigma^{|3|}$ contribution to the a_{2n} parameters is very small according to Eq. (5). The third column gives the $\sigma^{|M|}$ parameters obtained by fitting both curves simultaneously. The corresponding curve fits are shown in Fig. 2. Thus each alignment curve can be analyzed in terms of the same set of $\sigma^{|M|}$ parameters, providing a consistent check of the relative cross sections. The alignment effect is found to be large, with σ^0 being twice as large as $\sigma^{|3|}$. This may be explained on the basis of the potential curves, since the most likely coupling of the $^1F_3$ state and the $^1S_0$ state ($\Omega=0$) will occur through an avoided crossing in the $\Omega=0$ manifolds of both potential-energy surfaces, with Ω being the projection of the total angular momentum onto the internuclear axis.

TABLE I. Results of the least-squares fit of Eqs. (1) and (3). The numbers in parentheses are the error bars in the last digit given (± 1 standard deviation). The relative cross sections are normalized such that $\sigma^0+2\sigma^{|1|}+2\sigma^{|2|}+2\sigma^{|3|}=2J+1=7$.

	Parallel $\updownarrow\updownarrow\updownarrow$[a]	Perpendicular $\leftrightarrow\updownarrow\updownarrow$[a]	Parallel and perpendicular[b] $\updownarrow\updownarrow\updownarrow$	$\leftrightarrow\updownarrow\updownarrow$
a_0	0.956(4)	0.987(4)	0.957	0.991
a_2	0.182(6)	0.086(5)	0.185	0.077
a_4	0.082(6)	−0.020(6)	0.078	−0.038
a_6	−0.027(6)	0.042(6)	−0.031	0.045
σ^0	1.34(1)	1.46(2)	1.34(1)	
$\sigma^{\|1\|}$	1.24(2)	1.39(1)	1.25(1)	
$\sigma^{\|2\|}$	0.75(2)	0.82(3)	0.75(2)	
$\sigma^{\|3\|}$	0.84(2)	0.55(10)	0.83(2)	

[a]Parameters of Eqs. (1) and (3) obtained by fitting the two alignment curves of Fig. 2 individually.
[b]$\sigma^{|M|}$ parameters according to Eq. (3) with both measurements combined. The corresponding a_{2n} values are calculated with Eqs. (4) and (5). These fit curves are shown in Fig. 2.

In summary, we have studied the angular cross section dependence for an aligned $Ca(4s4f, ^1F_3)$ state colliding with He. Angular dependence up to rank-6 terms has been clearly demonstrated for the first time, in agreement with the total angular momentum $J=3$. Analysis in terms of cross sections $\sigma^{|M|}$ results in a large magnetic sublevel dependence. Although potential-energy surfaces are not yet available for this system, the alignment behavior can be understood intuitively in terms of an avoided crossing localized in the $\Omega=0$ manifolds. We are presently measuring energy-transfer alignment effects for the $Ca(^1F_3)$ state in collisions with the rare gases. These results will be presented [25].

We gratefully thank the National Science Foundation for generous support of this research.

*Quantum Physics Division, National Institute of Standards and Technology, Boulder, CO.

[1] L. Hüwel, J. Maier, and H. Pauly, J. Chem. Phys. **76**, 4961 (1982).
[2] J. M. Mestdagh, J. Berlande, P. de Bujo, J. Cuvellier, and A. Biner, Z. Phys. A **304**, 3 (1982).
[3] H. Schmidt, A. Bähring, E. Meyer, and B. Miller, Phys. Rev. Lett. **48**, 1008 (1982).
[4] A. Bähring, I. V. Hertel, E. Meyer, and H. Schmidt, Z. Phys. A **312**, 293 (1983).
[5] A. Bähring, I. V. Hertel, E. Meyer, W. Meyer, N. Spies, and H. Schmidt, J. Phys. B **17**, 2859 (1984).
[6] A. Bähring, E. Meyer, I. V. Hertel, and H. Schmidt, Z. Phys. A **320**, 141 (1985).
[7] G. Kircz, R. Morgenstern, and G. Nienhuis, Phys. Rev. Lett. **48**, 610 (1982).
[8] G. Nienhuis, Phys. Rev. A **26**, 3137 (1982).
[9] H. A. J. Meijer, T. J. C. Pelgrim, H. G. M. Heideman, R. Morgenstern, and N. Andersen, Phys. Rev. Lett. **59**, 2939 (1987); J. Chem. Phys. **90**, 738 (1989).

[10] W. Bussert, T. Bregel, J. Ganz, K. Harth, A. Siegel, M. W. Ruf, and H. Hotop, J. Phys. (Paris) Colloq. **46**, C1-199 (1985).

[11] W. Bussert, T. Bregel, R. J. Allan, M. W. Ruf, and H. Hotop, Z. Phys. A **320**, 105 (1985).

[12] M. O. Hale, I. V. Hertel, and S. R. Leone, Phys. Rev. Lett. **53**, 2296 (1984).

[13] W. Bussert and S. R. Leone, Chem. Phys. Lett. **138**, 269 (1987); **138**, 276 (1987).

[14] W. Bussert, D. Neuschäfer, and S. R. Leone, J. Chem. Phys. **87**, 3833 (1987).

[15] H. Hülser, E. E. B. Campbell, R. Witte, H. Genger, and I. V. Hertel, Phys. Rev. Lett. **64**, 392 (1990).

[16] R. L. Robinson, L. J. Kovalenko, and S. R. Leone, Phys. Rev. Lett. **64**, 388 (1990).

[17] R. L. Robinson, L. J. Kovalenko, C. J. Smith, and S. R. Leone, J. Chem. Phys. **92**, 5260 (1990).

[18] M. P. I. Manders, J. P. J. Driessen, H. C. W. Beijerinck, and B. J. Verhaar, Phys. Rev. Lett. **57**, 1577 (1986); **57**, 2472 (1986); Phys. Rev. A **37**, 3237 (1988).

[19] M. P. I. Manders, W. M. Ruyten, F. v.d. Beucken, J. P. J. Driessen, W. J. T. Veugelers, P. H. Kramer, E. J. D. Vredenbregt, W. B. M. van Hoek, G. J. Sandker, H. C. W. Beijerinck, and B. J. Verhaar, J. Chem. Phys. **89**, 4777 (1988).

[20] J. P. J. Driessen, F. J. M. van de Weijer, M. J. Zonneveld, L. M. T. Somers, M. F. M. Janssens, H. C. W. Beijerinck, and B. J. Verhaar, Phys. Rev. Lett. **62**, 2369 (1989); **64**, 2106 (1990); Phys. Rev. A **42**, 4058 (1990).

[21] A. G. Suits, H. T. Hou, and Y. T. Lee, J. Phys. Chem. **94**, 5672 (1990).

[22] C. Richter, D. Dowek, J. C. Houver, and N. Andersen, J. Phys. B **23**, 3925 (1990).

[23] I. V. Hertel, H. Schmidt, A. Bähring, and E. Meyer, Rep. Prog. Phys. **48**, 375 (1985).

[24] E. E. B. Campbell, H. Schmidt, and I. V. Hertel, Adv. Chem. Phys. **72**, 37 (1988).

[25] J. P. J. Driessen, C. J. Smith, and S. R. Leone, J. Phys. Chem. (to be published).

[26] A. Messiah, *Quantum Mechanics* (North-Holland, Amsterdam, 1961), p. 1068.